HIISI, NEW 18 GHZ ECRIS FOR THE JYFL ACCELERATOR LABORATORY*

H. Koivisto#, O. Tarvainen, T. Kalvas, K. Ranttila, P. Heikkinen, JYFL, Jyväskylä, Finland
D. Xie, LBNL, Berkeley, USA
G. Machicoane, NSCL, East Lansing, USA
T. Thuillier, LPSC, Grenoble, France
V. Skalyga, I. Izotov, IAP RAS, Nizhny Novgorod, Russia

Abstract

At the end of 2013 the Academy of Finland granted an infrastructure funding for the JYFL Accelerator Laboratory in order to increase beam intensities for the international user community. The primary objective is to construct a new high performance ECR ion source, HIISI (Heavy Ion Ion Source Injector), for the K130 cyclotron. Using room temperature magnets the HIISI has been designed to produce about the same magnetic field configuration as the superconducting ECRIS SUSI at NSCL/MSU for 18 GHz operation. An innovative structure will be used to maximize the radial confinement and demagnetization safety margin of the permanent magnets. The sextupole magnet is separated and insulated from the plasma chamber providing two advantages: 1) the permanent magnet can be cooled down to -10˚C to increase its coercivity and 2) at the same time to reach slightly higher radial field on the inner surface of the plasma chamber. Comprehensive simulations were performed with the radial heat load to analyse and address all the heat loads and temperature distribution on the permanent magnet. This information is crucial to define the maximum plasma heating power and the grade of the permanent magnets. In this article the magnetic field design of HIISI and detailed innovative scheme for sextupole magnet will be presented.

INTRODUCTION

Figure 1 shows the xenon ion beam intensities produced by high performance ECR ion sources. GTS [1], operating at 18 GHz frequency, is the best performing ECR ion source using room temperature magnets (resistive coils and permanent magnet sextupole), while VENUS [2] and SUSI [3] are fully superconducting ECR ion sources. The same performance level has also been achieved by fully superconducting SECRAL [4]. Although the great performance of superconducting ion sources meets and exceeds our goals, their construction costs greatly exceeds the available funding for the new JYFL ECR ion source leading to the choice of a room-temperature magnet ECRIS.

From the ion source performance point of view the most challenging requirement for HIISI is the production of highly charged heavy ion beams. For example, an intensity of about 10 nA for Xe^{44+} ion beam is needed to guarantee the requested beam energy and particle flux after the K130 cyclotron. This requirement is shown in Figure 1 by a red circle, which is beyond the performance of any present room-temperature magnet ECR ion source. The development of this new ECR ion source HIISI will enhance the high quality nuclear physics research at JYFL and potential for exciting discoveries in the future.

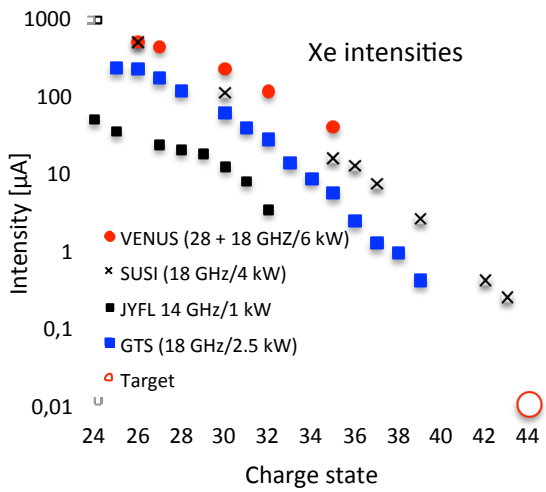

Figure 1: Intensities of Xe ion beams produced by different ECR ion sources. The red circle indicates the beam intensity of Xe^{44+} ion beam to be produced with the new ECRIS operated at 18 GHz.

MAGNETIC FIELD STRUCTURE

As Figure 1 shows, the performance of SUSI exceeds the desired intensity of Xe^{44+} ion beam when operated at 18 GHz with the microwave power of 4 kW. The magnetic field configuration of SUSI for the production of Ar^{12+} and Xe^{35+} ion beams are listed in Table 1 indicating that the intensive highly-charged ion beams can be produced with the magnetic field strengths in the range of: 2.5 – 2.8 T (B_{inj}), 1.2 – 1.5 T (B_{ext}), 1.1 – 1.35 T (B_{rad}) and about 0.45 T (B_{min}). All these field strengths agree well with the empirical source design criteria [5]. The

* This work has been supported by the EU 7th frame- work programme Integrating Activities - Transnational Access, project number: 262010 (ENSAR), the Academy of Finland under the Finnish Centre of Excellence Programme 2012- 2017 (Nuclear and Accelerator Based Physics Research at JYFL) and under the Finnish Research Infrastructure (FIRI) Programme of the Academy of Finland.
#hannu.koivisto@phys.jyu.fi

ISBN 978-3-95450-158-8

plasma chamber of SUSI is 100 mm in diameter with axial resonance surface length (cold electrons) varying between 110 – 145 mm. Although somewhat challenging these field configurations could be achieved with room temperature magnets and are the design basics for HIISI.

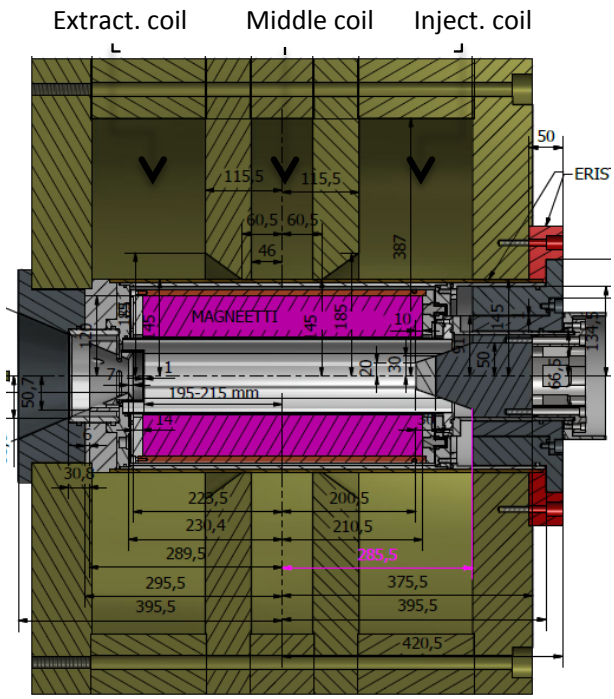

Figure 2: Layout of the JYFL 18 GHz ECRIS, HIISI.

Figure 2 shows the cross-sectional view of the new 18 GHz ECRIS HIISI. Each of the injection and extraction coils has 7 double pancakes with 20 radial turns. A middle coil of 3 similar double pancakes will be used for fine-tuning of the minimum-B (B_{min}). Table 2 shows the magnetic field configurations with different coil excitations, that are very close to the SUSI operation parameters at 18 GHz as shown in Table 1. The power consumption for generating these field configurations ranges between 137 kW – 216 kW. The axial magnetic field profile is shown in ref. [6].

Both tables show also the gradients of magnetic field (gradB) on the axial resonance points (for cold electrons). Several groups have observed the link between the magnetic field gradient and plasma instabilities: for more details see for example [7, 8]. For example, the operation experience with SUSI has shown that the ion beam becomes unstable when the gradient of magnetic field goes below 5 T/m but this threshold can be different for different ion source geometries. HIISI can be operated in single-frequency mode of either 18 GHz or 14 GH waves and also in multiple-frequency mode of 14 GHz and 18 GHz waves together with TWTA. In 14 GHz operation mode the power consumption of coils can be kept below 100 kW.

REFRIGERATED AND INSULATED SEXTUPOLE CHAMBER

Both the injection coil and the permanent magnet sextupole generate high demagnetizing fields on the permanent magnet blocks. To minimize the demagnetization, permanent magnet grade of N40UH, having B_{rem} and coercivity of 1.29 T and 1990 kA/m at 20˚C, respectively, has been chosen for constructing the sextupole magnet for HIISI. A comprehensive demagnetization analysis will be presented elsewhere in this proceeding [6]. According to the analysis a negligible permanent magnet volume exposes to demagnetizing field exceeding 1800 kA/m. Therefore safe operation is guaranteed as long as the magnet temperature will not exceed 20˚C.

The high coercivity of selected magnet material limits the remanence (B_{rem}) to 1.29 T. As a result, the radial field of 1.36 T (B_{rad}) shown in Table 1 is very difficult to reach. Two techniques have been studied in order to maximize B_{rad}: 1) new cooling scheme to minimize the gap between the plasma and inner surface of permanent magnet sextupole and 2) cooling of the permanent magnets to 0˚C or less.

Table 1: Intensities of Ar^{12+} and Xe^{35+} ion beams produced by SUSI at 18 GHz heating frequency with the shown magnetic field configurations.

Element	q	I [uA]	$P_{\mu w}$ [kW]	B_{rad} [T]	B_{inj} [T]	B_{min} [T]	B_{ext} [T]	gradB Inj [T/m]	gradB Ext [T/m]	Plasma Length
^{129}Xe	35+	16	3.2	1.36	2.8	0.46	1.56	6.6	5.9	115 mm
^{40}Ar	12+	730	3.8	1.06	2.5	0.43	1.19	6.8	5.6	142 mm

Table 2: Magnetic field configurations of HIISI designed for 18 GHz operation.

Pcoils [kW]	I_{inj}	I_{mid}	I_{ext}	B_{inj} [T]	B_{min} [T]	B_{ext} [T]	gradB Inj [T/m]	gradB Ext [T/m]	Plasma Length
216	1050	600	1050	2.51	0.43	1.52	6.3	6.3	132 mm
158	1000	300	820	2.48	0.42	1.33	6.1	6.1	143 mm
137	1000	210	680	2.48	0.41	1.18	6.2	5.5	157 mm

ISBN 978-3-95450-158-8

Plasma Chamber Cooling Scheme

The new cooling scheme of plasma chamber is presented in Figure 3. The plasma chamber and permanent magnets are fully separated by a vacuum insulated gap (about 1.5 mm). The water-cooling channel is located by the side of the plasma flux, i.e both sides of radial magnetic pole. This makes it possible to decrease the wall thickness of plasma chamber on the magnetic pole to about 2.5 mm. Such a design leads to a total distance of 4 mm between the plasma chamber inner wall and permanent magnet inner surface. The plasma chamber is placed inside a refrigerated sextupole chamber, which is shown in Figure 7.

The plasma chamber is not physically in direct contact with the permanent magnet blocks and consequently its temperature does not play a critical role regarding the demagnetization of the permanent magnet blocks. In this design the total heat load on the permanent magnet blocks comes from the heat radiation, heat transfer by the residual molecules inside the vacuum gap and by the heat conduction from the support structure of the sextupole chamber. Although the heat load is small it will increase the temperature of the magnets and these effects have to be taken into account in the design of the cooling of the sextupole magnet. These studies are presented elsewhere in these proceedings by T. Kalvas [6].

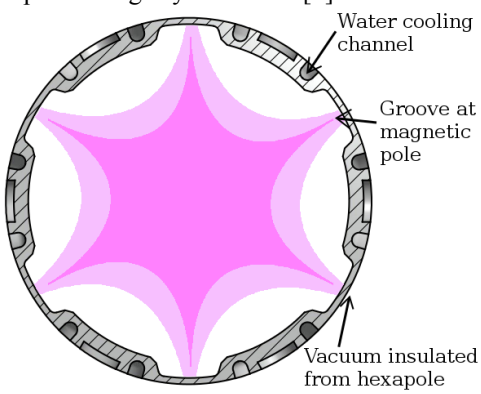

Figure 3: Plasma chamber structure for maximizing radial field strength.

Temperature Distribution and Maximum Microwave Power

The temperature distribution of the plasma chamber is needed for two reasons: 1) to define the heat load and temperature distribution of permanent magnets and 2) to define the maximum temperature of the aluminium chamber. The first information is needed in order to design the cooling of the permanent magnets and to choose the magnet grade, while the latter one to define the maximum operating microwave power. Based on the magnetic symmetry the chamber has been divided to 3 symmetric sectors to minimize time needed for the simulations. Figure 4 shows the temperature distribution (1/12 sector) on the surface of the plasma chamber wall when an electron flux carrying a total power of 6 kW is lost radially. According to our plasma flux simulations about 80 % of the microwave power will be directed to radial loss cones (see [6]). As Figure 4 shows the total radial heat load of 6 kW for the given geometry will result in a maximum temperature of around 410 K on the plasma chamber wall. In the simulations the cooling water temperature of 300 K was used. The total wall thickness and width of the groove was 2.5 mm and 16 mm, respectively. In order to avoid the aging of aluminium (deterioration of strength properties) the maximum temperature should be kept below 370 K (100 ˚C). Consequently, the total microwave power fed into the plasma chamber has to be kept below 5 kW. Here it is assumed that 80 % of the power is directed toward the radial poles corresponding to the radial power load of 4 kW. This value is not exceeded by using simultaneously two Klystrons and TWTA having the power of 2.4 kW and 500 W, respectively. Here it is assumed that the transmission losses are 10 % or more.

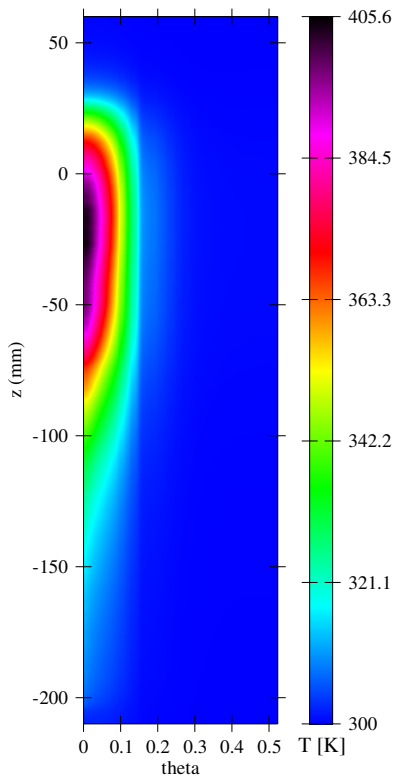

Figure 4: Temperature distribution on surface of the plasma chamber. Total radial power flux of 6 kW was used in the simulations.

Refrigerated Permanent Magnets

It is a well-known fact that the coercivity and the remanence magnetic field B_{rem} of permanent magnets decrease with increasing temperature. This effect was studied at JYFL [9] by cooling of the magnets and by defining the value of B_{rem} as a function of temperature.

ISBN 978-3-95450-158-8

The experimental behaviour of remanence field is shown in Figure 5. The experiments were performed using the permanent magnet grade of N48 having the values of 1.42 T and 1353 kA/m for B_{rem} and coercive force, respectively. This magnet grade is used for the sextupole of the JYFL 14 GHz ECRIS. The field increased from 1.4 T (at room temperature) up to 1.57 T by using liquid N2 cooling. A cryogenic sextupole scheme has been studied also by LSPC ion source group by simulations [10]. This property of permanent magnets will be studied and tested with HIISI.

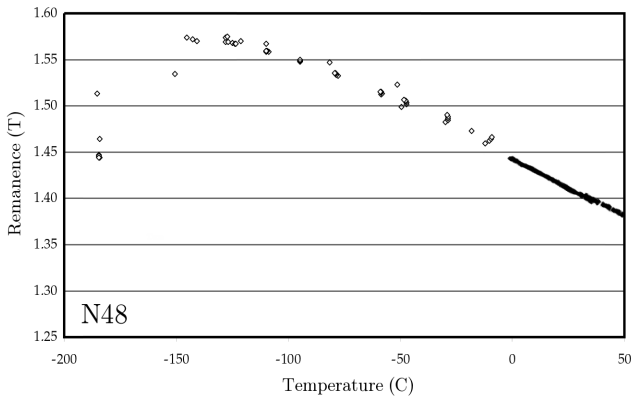

Figure 5: Remanence magnetic field B_{rem} of grade N48 permanent magnet experimentally defined as a function of temperature [9].

Figure 6 shows the demagnetization curves and coercive force for selected magnet grade (N40UH) at different temperature. As mentioned above the demagnetization analysis has shown a negligible volume of the permanent magnets experiences demagnetizing stress exceeding 1800 kA/m. Consequently, the magnets are in safe operation point as long as their temperature is kept at around 20˚C (or below). The extra cooling will increase B_{rad} and especially the coercive force of the magnets. A mechanical stress analysis indicated that the sextupole magnet configuration can be cooled down to -10˚C without any irreversible damages or reaching the yield point of sextupole chamber made of aluminum (see Figure 7).

As a consequence of mechanical stress analysis the design goal is to cool the permanent magnet down to -10˚C. This would strongly improve the coercive force making it possible to use other grade of permanent magnet material – for example N48. The effect of cooling and use of other magnet grade is shown in Table 3. The configuration numbers 1-7 are related to 24-segment Halbach and configuration number 8 to 36-segment Halbach. The first sextupole configuration will be realized by using a 24 -segment offset [11] Halbach structure having the gap of 4 mm and magnet grade of N40UH (configuration number 4 in Table 3). This will result in B_{rad} of 1.24 T/1.28 T depending on the temperature of the permanent magnets (20˚C/-10˚C). The latter value, which is reached at -10˚C, fulfils the scaling rule for sextupole field. However, it does not fully reach the B_{rad} value, shown in Table 1, needed for the production of high intensity Xe^{35+} ion beam.

Table 3: Value of B_{rad} with different configurations.

Config. No	Gap [mm]	T [˚C]	B_{rem} (at 20˚C) [T]	B_{rad} [T]
1	3	20	1.29	1.29
2	4	20	1.29	1.24
3	5	20	1.29	1.19
4	**4**	**-10**	**1.29**	**1.28**
5	4	-30	1.29	1.31
6	4	-30	1.32	1.34
7	4	-30	1.42	1.44
8	4	-30	1.42	1.51

As a next step, when the operation with the refrigerated sextupole structure at -10˚C is fully developed and found reliable, the sextupole structure will be realised by using other grade of magnet material (N48 grade shown in Table 1, Config. No 7-8). In addition to this and further development of cooling (for example down to -30˚C) the sextupole field up to 1.5 T could be reached.

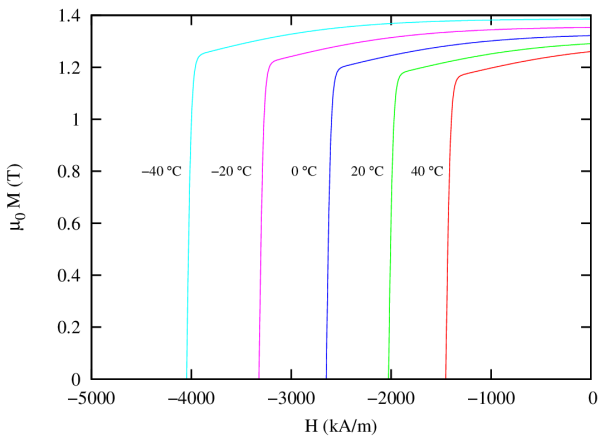

Figure 6: Demagnetization behaviour of N40UH permanent magnet as a function of temperature.

Figure 7 shows the configuration designed for the cooled and vacuum insulated permanent sextupole magnet. The plasma chamber is situated inside the sextupole chamber, which is nested in a pumping chamber. Using this arrangement the permanent sextupole magnet is in rough vacuum and exposed to following heat loads: 1) heat radiation from surrounding structures, 2) power flux caused by the residual gas and 3) heat conduction via support structure. Although the microwave power will not exceed 5 kW the temperature distribution shown in Figure 4 has been used for the afore-mentioned simulations for some extra safety margin. The comprehensive heat load and temperature distribution simulations are presented in [6] confirming that this scheme for the cooling of sextupole magnet is feasible.

ISBN 978-3-95450-158-8

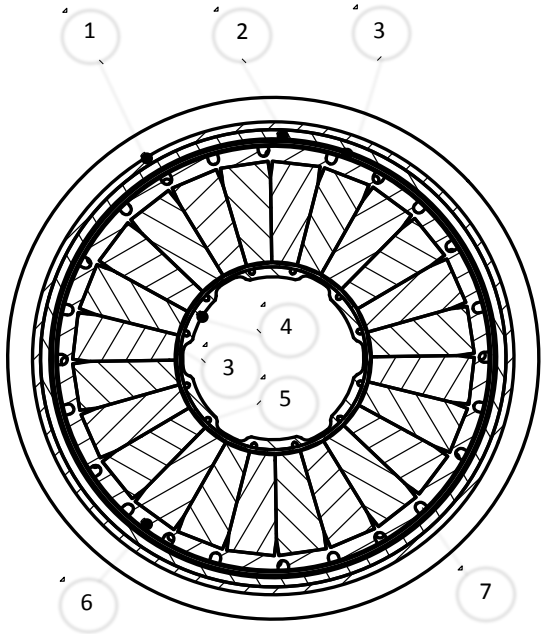

Figure 7: Plasma chamber inside the sextupole chamber and sextupole pumping chamber: 1) Insulator, 2) Sextupole pumping chamber, 3) Rough vacuum, 4) Plasma chamber, 5) Plasma chamber cooling line, 6) Sextupole chamber, 7) Sextupole chamber cooling line.

The design project was started in the beginning of 2014. In fall 2014 we are now ready to start the work for the detailed drawings. The first components will be ordered by the end of 2014 while the main components for the production of magnetic field will be ordered by summer 2015. Site construction will be started during the fall of 2015 and source commissioning is expected by summer 2016.

REFERENCES

[1] D. Hitz, A. Girard, K. Serebrennikov, G. Melin, D. Cormier, J. M. Mathonnet, and J. Chartier, Rev. Sci. Instrum, Vol 75 (5), (2004), p. 1403.
[2] C. M. Lyneis, D. Leitner, S. R. Abbott, R. D. Dwinell, M. Leitner, C. S. Silver, and C. Taylor, Rev. Sci. Instrum., Vol. 75 (5), (2004), p. 1389.
[3] P. A. Zavodszky et. al., Rev. Sci. Instrum., Vol. 79, (2008), p. 02A302.
[4] H.W. Zhao, et al., Rev. Sci. Instrum., Vol. 77, (2006), p. 03A333.
[5] D. Hitz, A. Girard, G. Melin, S. Gammino, G. Ciavola, and L. Celona, Rev. Sci. Instrum. **73**, (2002), p. 509.
[6] T. Kalvas et al., this proceeding.
[7] O. Tarvainen et al., Plasma Sources Sci. Technol. 23 (2014), p. 025020.
[8] G. Machicoane, private discussion.
[9] P. Frondelius, Master thesis, Department of Physics, University of Jyväskylä, 2005.
[10] T. Thuillier, T. Lamy, C. Peaucelle and P. Sortais, Rev. Sci. Instrum., Vol. 81, (2010), p. 02A316.
[11] P. Suominen, O. Tarvainen, H. Koivisto and D. Hitz, Rev. Sci. Instrum., Vol. 75 (1), (2003), p. 59.

ISBN 978-3-95450-158-8